Distortion Correction in DW-EPI using an Extended PSF Method with a Reversed Gradient Approach

Myung-Ho In[1], Oleg Posnansky[1], Erik B. Beall[2], Mark J. Lowe[2], and Oliver Speck[1,3]
[1]*Biomedical Magnetic Resonance, Otto-von-Guericke University, Magdeburg, Germany, Magdeburg, Germany,* [2]*Radiology, Imaging Institute, Cleveland Clinic, Cleveland, OH, USA, OH, United States,* [3]*Leibniz Institute for Neurobiology, Magdeburg, Germany, Magdeburg, Germany*

INTRODUCTION In echo-planar imaging (EPI), compressed distortion is a more difficult challenge due to loss of spatial information. To resolve this problem, two EPIs with opposite phase-encoding (PE) polarity were acquired and combined after distortion correction [1,2]. For more accurate distortion correction, a modified point spread function (PSF) mapping method [3] was chosen. A single PSF reference acquisition was extended such that it could be used for distortion correction of EPIs with opposite PE polarity without an additional PSF reference scan [4]. In this study, the accuracy of the proposed method was further evaluated in distortion-corrected data using both forward (F) and reverse (R) phase-encoded PSF reference data. In addition, we propose a suitably weighted combination of the two distortion-corrected images that accounts for the different amount of spatial information in each image.

METHODS EPI-PSF-based weighting maps for summation of the EPI pair: In ref. [3], a distortion-corrected EPI image $I_c(s)$ can be written as:

$$I_c(s) = \int I(y)H_c(y,s)dy = \int I_c(y,s)dy. \quad (1)$$

This is the convolution product of a distorted EPI $I(y)$ and the EPI-PSF kernel $H_c(y,s)$. After distortion correction by the EPI-PSF kernel, the signal will be increased in previously stretched regions due to image compression and vice versa in the regions with compressed distortions. Since the signal is changed by geometric distortion correction using the EPI-PSF kernel $H_c(y,s)$, it includes a modulation function to correct the signal intensity. An integration of the EPI-PSF kernel along the y-axis yields a modulation function as a weighting map $W(s)$ in this study:

$$W(s) = \int H_c(y,s)dy. \quad (2)$$

We assume that the spatial information in the originally stretched regions is more reliable than the information in the compressed regions [5]. Therefore, instead of simply averaging the distortion-corrected forward $I_{c,F}(s)$ and reverse $I_{c,R}(s)$ EPIs, a weighted average is proposed in this study in order to generate the optimally combined distortion-free image $I_{WA}(s)$:

$$W_{WA}(s) = (W_F(s)I_{c,F}(s)+W_R(s)I_{c,R}(s))/(W_F(s)+W_R(s)) \quad (3)$$

Experiments: All scans were performed on a 7T scanner (Siemens Healthcare, Erlangen, Germany) using a 32 channel phase-array head coil (Nova Medical, Wilmington MA, USA). (I) Pairs of EPIs and PSF data with opposite PE polarity were acquired. The imaging parameters were: 12 axial slices, slice thickness=1.2mm, TR/TE=2000/54 ms, BW=1544 Hz/pixel, FOV=224 mm^2, matrix size=180^2, partial Fourier=6/8, grappa factor=3. A pair of EPI-PSF kernels, which were applied to the corresponding pair of EPIs for distortion correction, was obtained from each of the forward and reverse phase-encoded PSF reference data and two pairs of distortion-corrected images were obtained using the two PSF data. In order to validate the correction quality, the distortion-corrected images were subtracted from each other. (II) *In-vivo* diffusion tensor imaging (DTI) experiments were performed. A PSF dataset with forward PE and pairs of diffusion weighted EPI (DW-EPI) with opposite PE polarity were acquired, corresponding to two averages in regular acquisitions. The imaging protocols were identical to the first experiment with the exception of TR/TE = 5910/56 ms and the use of 80 axial slices to cover the entire brain. The number of diffusion directions for DW-EPI was 30 (b-value = 1000 s/mm^2). The forward and extended EPI-PSF kernels were obtained from the forward PSF reference data to correct distortions in both DW-EPIs with opposite PE polarity. Every distortion-free image was finally generated by weighted summation of the two distortion-corrected images using the proposed weighting factors calculated from the EPI-PSF pair according to Eq. 3. Based on the distorted (F and R), distortion-corrected (F and R), and combined DW-EPIs, five fractional anisotropy (FA) maps were calculated after eddy-current correction and registration, and compared to evaluate the spatial accuracy. The FA map calculation, eddy current correction, and registration were carried out in FSL [6].

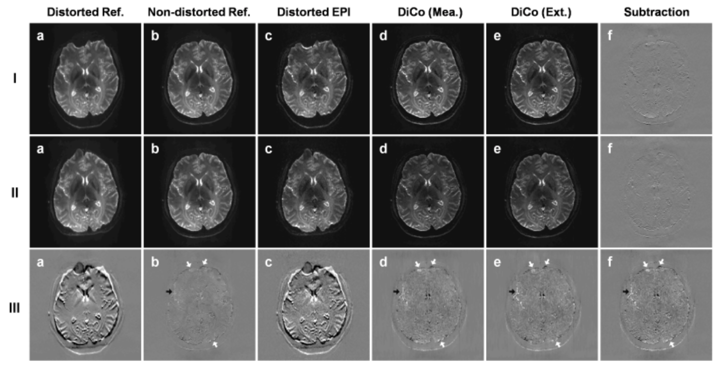

Fig. 1 Distortion correction (DiCo) with forward (row I) and reverse (row II) phase-encoded EPIs and their differences (row III): (a and b) distorted and non-distorted reference (Ref.) images calculated from the 3D PSF data, (c) distorted EPI image, (d and e) the distortion-corrected EPI images corrected by the EPI-PSF kernels calculated from the corresponding measured (Mea.) and extended (Ext.) PSF data with forward (row I) and reverse (row II) PE polarity, respectively. (I-f and II-f) subtracted images between (d) and (e), and (III-f) a subtracted image between (I-d) and (II-e), which is the proof of high quality result obtained by the proposed method.

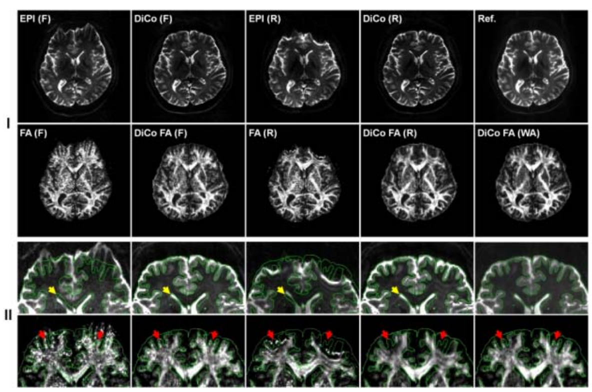

***Fig. 2** Forward (F) and reverse (R) spin-echo EPIs without and with DiCo (I upper row) and the corresponding FA maps (I bottom row). A final FA map was calculated after weighted average (WA) of the two distortion corrected DW-EPIs using the proposed weighting maps. Green contours calculated from the reference image (Ref.) were overlaid onto the enlarged images (II) of the anterior regions of the full FOV images (I).*

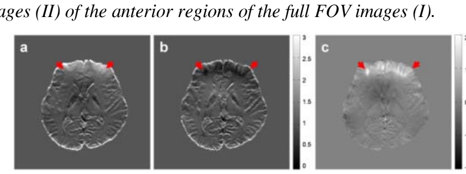

***Fig. 3** The EPI-PSF kernel based weighting maps and the ratio map: two weighting maps, $W_F(s)$ (a) and $W_R(s)$ (b), are calculated respectively from the forward and reverse EPI-PSF kernel using Eq. 2 and the ratio (c) is shown in logarithmic scale using the equation of $\log_e(W_F(s)/W_R(s))$.*

RESULTS AND DISCUSSION The geometrical differences between the forward and reverse EPI images are significantly reduced after the proposed distortion correction (Figs. 1). Although some residual differences remain in strongly distorted regions (see white arrows) as well as in the ventricle and arterial (see black arrows) regions (Figs. 1IIId-f), the differences were not changed even if either the measured (Fig. 1IIId), extended (Fig. 1IIIe), or proposed method (Fig. 1IIIf) were used for the distortion correction. In addition, very similar results (Fig. 1IIIb) were obtained by subtraction between the non-distorted forward (Figs. 1I-b) and reverse reference images (Figs. 1II-b), which were respectively calculated from the forward and reverse PSF data. Therefore, the extended PSF method image discrepancies are primarily due to acquisition-related artifacts (e.g. motion, flow), rather than the distortion correction process. After distortion correction, the EPIs and FA maps matched well with the reference image without distortions (Fig. 2). Although loss of spatial information due to compressions cannot be recovered by the distortion correction (DiCo FA (R) map in Fig. 2II bottom row), the proposed weighted combination of EPIs allows generating a final FA map with efficient spatial information (DiCo FA (WA) in Fig. 2II bottom row). Compared to the reverse EPI image, the forward EPI image introduces 8 times higher contribution ($\log_e 8$=2.08) to the combined image in the anterior regions (see red arrows in Fig. 3) and lower contribution near ventricle regions when the combination process is performed. Thus, the combination process primarily accounts for the effects of PSF shifts, not blurring (Fig. 3c).

CONCLUSION The results demonstrate that the proposed method corrects distortion of EPI data with both PE directions very efficiently with very little remaining spatial errors. The extended PSF method was applied to DTI acquired with both PE directions to perform a fair data analysis and interpretation.

REFERENCES **[1]** JL Andersson et al., *Neuroimage*2003; 20:870-888 **[2]** D Holland et al., *Neuroimage*, 2010; 50:175-183 **[3]** MH In and O Speck, *MAGMA*, 2012; 25(3):183-92 **[4]** MH In et al., ISMRM 2013 **[5]** S Skare and R Bammer, ISMRM 2010 **[6]** FSL, http://fsl.fmrib.ox.ac.uk/fsl/

ACKNOWLEDGEMENTS Grant support by DFG-grant (SP632-4).